Electromagnetic and Thermal Behaviors of Multilayer Anisotropic Composite Materials

Samir Bensaid, Didier Trichet, and Javad Fouladgar

Institut de Recherches en Electrotechnique et Electronique de Nantes Atlantique (IREENA), 44602 Saint-Nazaire cedex, France

A methodology based on shell elements, to study the electromagnetic and thermal behavior of multilayered anisotropic conductive composite materials, is presented. The anisotropic behavior and orientation of each layer of the composite material has been taken into account. The model is validated with experimental results. It is then applied to study the induction heating of composite materials, and also to detect the delamination in these materials.

***Index Terms*—Delamination, induction heating, multilayer composite material, shell elements.**

I. Introduction

COMPOSITE materials have benefited from a remarkable growth in manufacturing industries such as aeronautic, aerospace, and automobile. Carbon fibers composites have superior specific mechanical properties compared to conventional metallic materials. To form a composite sheet, carbon fibers are immerged in a thin layer of resin. Several layers are then assembled together with different fibers orientations to achieve the required thickness and the mechanical strength. In recent years, several works have been realized, carrying a considerable interest in induction heating [1]–[4] and structural monitoring [5], [7]–[9]of carbon fiber composite materials.

Due to the important number of carbon fibers impregnated in each layer, it is very difficult to take into account the real geometry in the simulation. The composite layer is then replaced by a homogenized one [1], [2]. Moreover, as the composite sheets have a small thickness compared with their other dimensions, shell elements can be used to reduce the number of unknowns. In our previous work [1], the case of three-dimensional (3-D) induction heating simulation of composite plate with equivalent anisotropic conductivities has been presented. It was shown that induction heating has best performance when the inductor currents' direction is in the low conductivity direction of the composite plate. This is verified only for single layer and plates of anisotropic composite material that has the same layer orientations. This model, however, does not work for the multilayer composite sheet with different fibers orientation in each layer.

In this work, we present a 3-D induction heating simulation model of a multilayer anisotropic composite materials. The real geometry of multilayer composite materials with equivalent anisotropic individual layer is taken into account. A global equivalent model is then introduced to take into account the different fibers' orientations. The model is validated with experimental results.

II. Problem Formulation

The electrical and thermal conductivities $(\sigma_{\mathrm{i}}, \lambda_{\mathrm{i}})$ of the layers are anisotropic and have a tensor form. Due to the small polymer gap between the layers, electrical conductivity in z direction is considered null

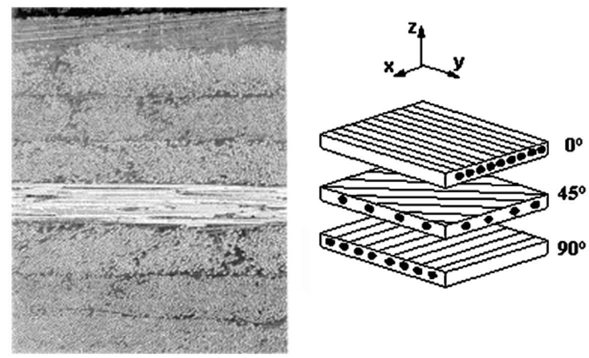

Fig. 1. Laminate anisotropic composite materials.

$$\sigma_i = \begin{pmatrix} \sigma_{xx_i} & \sigma_{xy_i} \\ \sigma_{yx_i} & \sigma_{yy_i} \end{pmatrix} \tag{1}$$

$$\lambda_i = \begin{pmatrix} \lambda_{xx_i} & \lambda_{xy_i} & 0 \\ \lambda_{yx_i} & \lambda_{yy_i} & 0 \\ 0 & 0 & \lambda_{z_i} \end{pmatrix}. \tag{2}$$

Shell elements are introduced in [6] to solve the 3-D electromagnetic problem on thin plate for isotropic materials, and have been generalized for an anisotropic conducting plate in [1]. One considers in the following calculus a multilayered composite plate with p equivalent anisotropic layers (Fig. 2). To obtain the electromagnetic shell elements formulation, one follows the following stages.

A. Electromagnetic Problem in the Layer i

To have the analytic solution of the magnetic field in the layer i, one solves the following equation system:

$$\begin{cases} \dfrac{d^2H_x(z)}{dz^2} - j\omega\mu\cdot\sigma_{yy_i}H_x(z) = j\omega\mu\cdot\sigma_{yx_i}H_y(z) \\ \dfrac{d^2H_y(z)}{dz^2} - j\omega\mu\cdot\sigma_{xx_i}H_y(z) = j\omega\mu\cdot\sigma_{xy_i}H_x(z) \end{cases} \tag{3}$$

with the following boundary conditions:

$$\begin{cases} \boldsymbol{H}\left(\frac{e_i}{2}\right) = \boldsymbol{H}_i \\ \boldsymbol{H}\left(-\frac{e_i}{2}\right) = \boldsymbol{H}_{i+1} \end{cases} \tag{4}$$

where e_i is the thickness of the layer i.

Digital Object Identifier 10.1109/TMAG.2006.870926

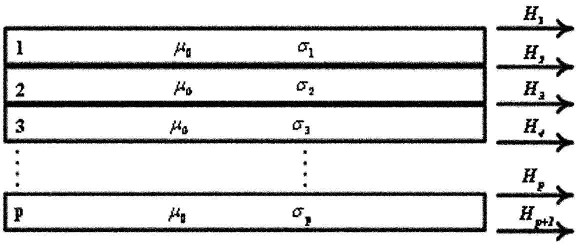

Fig. 2. Shell multilayers representation.

By introducing the analytic solution of the magnetic field in Faraday's law combined with the local form of Ohm's law, one obtains the anisotropic surface impedance description of each layer [1]:

$$\begin{pmatrix} \boldsymbol{E}_i \\ \boldsymbol{E}_{i+1} \end{pmatrix} = \mathbf{n} \times \begin{pmatrix} \alpha_i & -\beta_i \\ \beta_i & -\alpha_i \end{pmatrix} \begin{pmatrix} \boldsymbol{H}_i \\ \boldsymbol{H}_{i+1} \end{pmatrix} \tag{5}$$

where $\mathbf{n}$ is the normal vector and α_i with β_i are the tensors coefficients depending on the tensors of conductivity σ_i, the permeability μ of the layer, and the angular frequency of the magnetic field ω [1].

B. Electromagnetic Problem in the Assembled Layers

For an anisotropic composite plate of p layers one obtains the p anisotropic surface impedance equations (5). To have the global anisotropic surface impedance description, the intermediate magnetic fields $(H_1 \ldots H_p)$, and electrical fields $(E_1 \ldots E_p)$ are eliminated successively to obtain

$$\begin{pmatrix} \boldsymbol{E}_1 \\ \boldsymbol{E}_{p+1} \end{pmatrix} = \mathbf{n} \times \begin{pmatrix} \alpha_{1p} & -\beta_{1p} \\ \beta_{p1} & -\alpha_{p1} \end{pmatrix} \begin{pmatrix} \boldsymbol{H}_1 \\ \boldsymbol{H}_{p+1} \end{pmatrix} \tag{6}$$

where $(\alpha_{1\mathrm{p}}, \alpha_{\mathrm{p}1})$ and $(\beta_{1\mathrm{p}}, \beta_{\mathrm{p}1})$ are the tensors coefficients that appear in the finite-element formulation. This procedure is illustrated by **direct algorithm** of Fig. 3.

The tangential magnetic fields on both sides of the composite plate according to reduced scalar potential (ϕ) are written as

$$\begin{pmatrix} \boldsymbol{H}_1 \\ \boldsymbol{H}_{p+1} \end{pmatrix} = \begin{pmatrix} \boldsymbol{H}_{js} - \mathbf{grad}_s(\phi_1) \\ \boldsymbol{H}_{js} - \mathbf{grad}_s(\phi_2) \end{pmatrix} \tag{7}$$

where $\mathbf{H}_{js}$ is the source field, calculated by Biot and Savart's law.

The finite-element formulation in side 1 of the general problem (Fig. 4) is written as [1], [6]

$$\begin{aligned} &\frac{1}{jw} \int_\Gamma \mathbf{grad}_s w \cdot (\alpha_{1p} - \beta_{1p}) \cdot \begin{pmatrix} \mathbf{grad}_s(\phi_1) \\ \mathbf{grad}_s(\phi_2) \end{pmatrix} \cdot d\Gamma \\ &\quad + \int_{\Omega_1} \mu \cdot \mathbf{grad}\, w \cdot \mathbf{grad}(\phi_1) d\Omega = \int_\Gamma \mu w \boldsymbol{H}_j \cdot \boldsymbol{n}_1 d\Gamma \\ &\quad + \frac{1}{jw} \int_\Gamma \mathbf{grad}_s w (\alpha_{1p} - \beta_{1p}) \cdot \boldsymbol{H}_j d\Gamma. \end{aligned} \tag{8}$$

The other equation corresponding to the side "2" of the shell is obtained by permuting of the index 1 and 2 of normal vector n and reduced scalar potential ϕ [6].

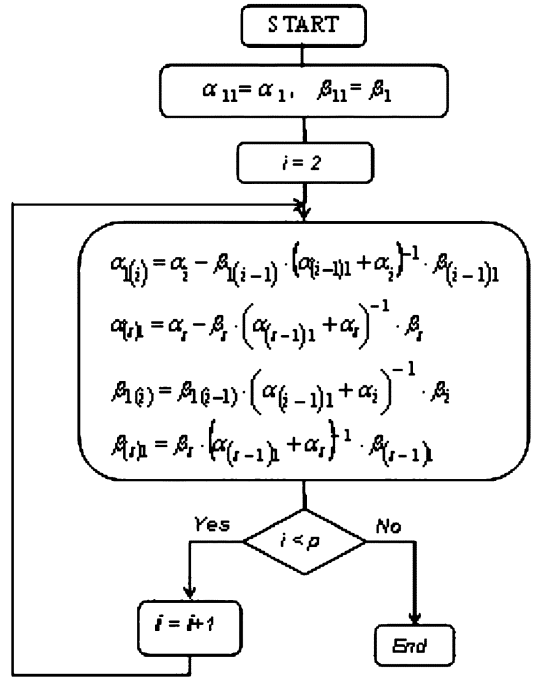

Fig. 3. Direct algorithm.

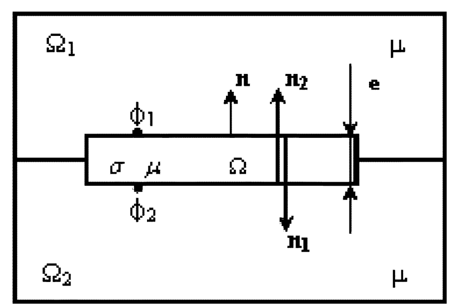

Fig. 4. General representation of shell elements.

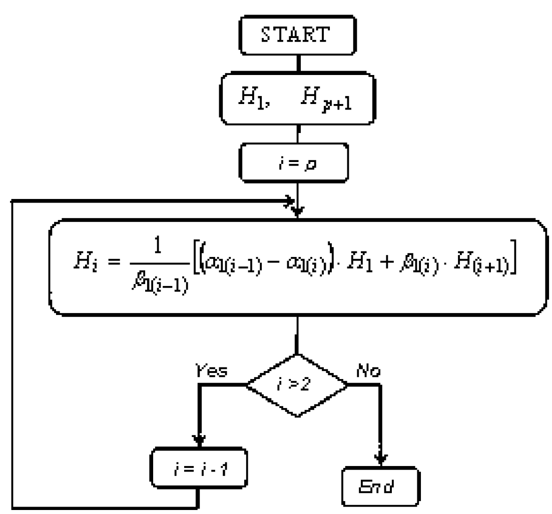

Fig. 5. Inverse algorithm.

The differences of electrical conductivity of each layer make difficult to calculate the heat source in the volume of the composite plate. To solve this difficulty, one calculates the interlayer magnetic field $H_1 \ldots H_{\mathrm{p}}$ using the **inverse algorithm** described in Fig. 5. The current density and the heat source in the volume

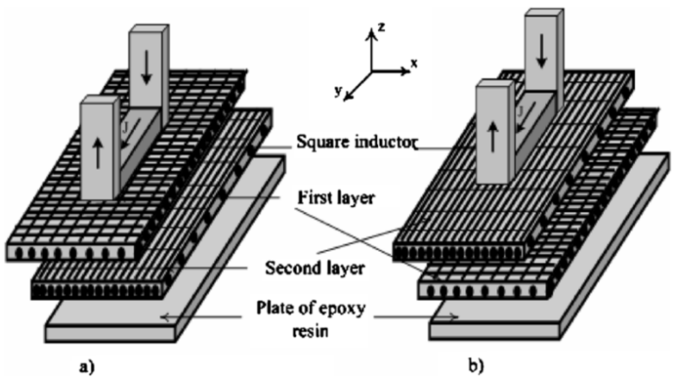

Fig. 6. Experimental setup. (a) Case I. (b) Case II.

of each layer can then be computed from the interlayer magnetic fields.

The heat source density P_i in the volume of layer i is calculated using the following equation:

$$P_i = \boldsymbol{J}_i^t \cdot \boldsymbol{E}(i) = \boldsymbol{J}_i^t \cdot \sigma_i^{-1} \cdot \boldsymbol{J}_i \tag{9}$$

with

$$\boldsymbol{J}_i = \mathbf{rot}\boldsymbol{H}(i). \tag{10}$$

$\boldsymbol{J}_i$ is the current density induced in the layer "i."

C. Thermal Problem

The thermal problem is solved only in the composite plate. The equation to be solved is written as [1]

$$\rho_i C_{p_i} \frac{\partial T}{\partial t} + \mathrm{div}(-\lambda_i \cdot \mathrm{grad}T) = P_i \tag{11}$$

with the Fourier boundary condition

$$-\lambda_i \cdot \frac{\partial T}{\partial \boldsymbol{n}} = h \cdot (T - T_a) \tag{12}$$

where λ_i is the thermal conductivity, ρ_i is the volumetric masse, C_{p_i} is the specific heat, h is the convective coefficient, P_i is the heat source density calculated before, T is the temperature in layer i, and T_a is the ambient temperature.

The mode of heat transfer between the layers is only by conduction. To solve the thermal equation, a 3-D finite-element method is used.

For all cases, the 3-D electromagnetic and thermal formulations are solved in a Matlab workspace.

III. Simulated and Experimental Results

A. Experimental Setup

The composite plate used in this experimentation is composed of two layers. The x, y conductivities of first layer are $(\sigma_{\mathrm{xx1}} = 2\sigma, \sigma_{\mathrm{yy1}} = \sigma, \sigma_{\mathrm{xy1}} = \sigma_{\mathrm{yx1}} = 0)$ and of the second layer are $(\sigma_{\mathrm{xx2}} = \sigma, \sigma_{\mathrm{yy2}} = 2\sigma, \sigma_{\mathrm{xy2}} = \sigma_{\mathrm{yx2}} = 0)$. The inductor used has a rectangular form with one turn; the current circulates in the specified direction of Fig. 6.

The induction generator gives the current of 180 A, and an electromagnetic frequency of 190 kHz. The air gap between the inductor and the load is 5.2 mm. The temperatures of the load were measured by means of thermocouples using a data acquisition device. An epoxy resin plate is heated by the two assembled layers (Fig. 6).

Fig. 7(a) and (b) represents the simulated and measured temperatures of two points below the epoxy resin plate.

A good agreement is obtained between simulated and measured temperatures in the load, with difference of 1.9%.

B. Layer Orientation

In order to see the influence of the layer orientation in the induction heating of multilayer composite materials, two cases are considered in the experimental setup. In the Case I, the inductor is above the first layer [Fig. 6(a)], whereas in Case II, the inductor is placed above of the second layer [Fig. 6(b)].

The experiments and simulations show that the composite plate is more heated in Case I than in Case II [Fig. 7(a) and (b)].

In order to see more comparison between different cases of fiber orientations in the two layers, the power source induced in the volume of the composite material is calculated for various cases (Table I).

With simulations, one can predict the optimal position of the inductor, in order to have a maximum of energy transfer.

The layer orientations in composite material have a great influence on the temperature distribution, and the solution exposed should be taken into account.

C. Delamination

Detection of delamination cracks in laminated composite is very important to improve structural reliability. This requires health monitoring technologies. In the literature, several techniques based on the electrical conductivity measurement are employed to detect delamination in laminate carbon fiber reinforcement thermoplastic. Among them, one quotes the electrical potential technique [7], the eddy-current method [8], and the electric resistance change method [9].

With the proposed approach, several induction heating simulation cases are investigated. It was noticed that if near the inductor (in the x–y axes) an insulating area of 12 mm^2 is incorporated in the composite sheet, local temperature elevation can be detected on the external surface of the sheet at the top of the insulating zone (Fig. 8). This confirms the possibility to use the new developed model to detect the delamination.

For this application, the continuous induction heating and infrared camera are required.

IV. Conclusion

In this work, a 3-D anisotropic shell element of multilayer composite materials is presented. The anisotropic character and the fibers orientation of each layer in the composite material are taken into account.

One has shown that the layer orientation has a great impact on the induction heating of multilayer composite materials. The method can be applied to detect the delamination in composite materials.

With the exposed method, one can also predict the optimal position of the inductor in order to have the best performance of heating for the desired applications.

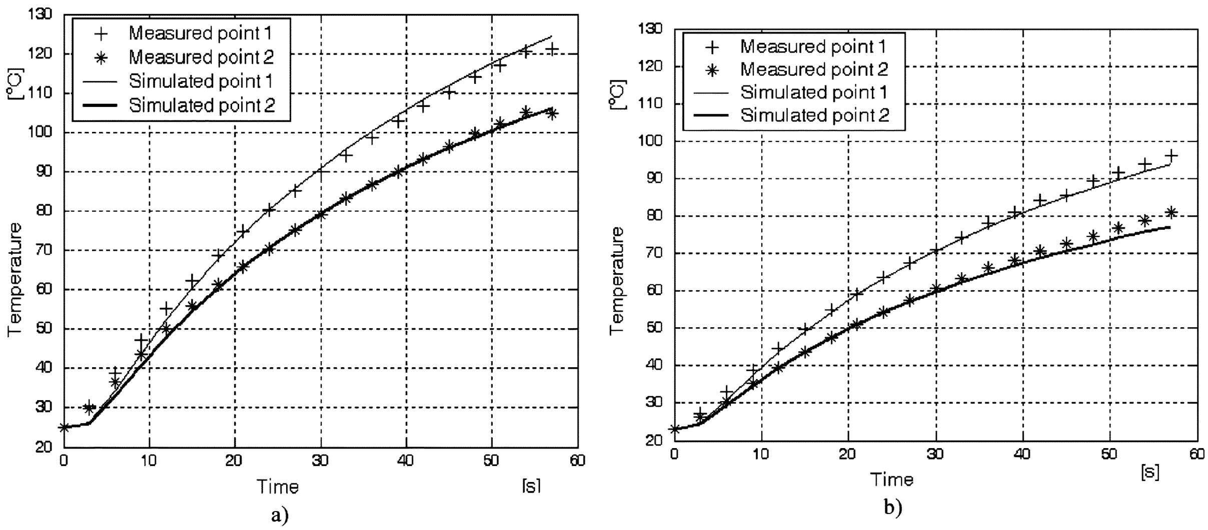

Fig. 7. Measured and simulated temperature evolution. (a) Case I. (b) Case II.

TABLE I
UNITS FOR MAGNETIC PROPERTIES

Fiber orientations	0-π/2	π/2-0	0-0	π/2-π/2	π/4-π/4
Induced power [Watt]	40.5	21.1	38.9	21.7	29.7

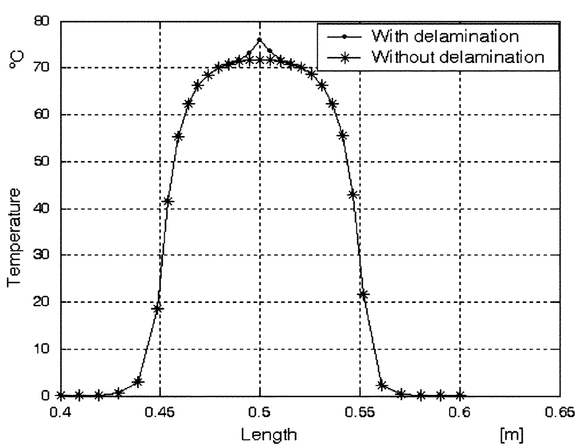

Fig. 8. Temperature distribution with and without delamination.

This method has been validated with an experimental case.

REFERENCES

[1] S. Bensaid, D. Trichet, and J. Fouladgar, "3-D simulation of induction heating of anisotropic composite materials," *IEEE Trans. Magn.*, vol. 41, no. 5, pp. 1568–1571, May 2005.

[2] D. Trichet, "Contribution à la modélization, à la conception et au développement du chauffage par induction des matériaux composites," Thèse de doctorat, école doctorale sciences pour l'ingénieur de Nantes, Jan. 2000.

[3] A. K. Miller, C. Chang, A. Payne, M. Gun, E. Menzei, and A. Peled, "The nature of induction heating in graphite-fiber, polymer-matrix composite materials," in *SAMPE J.*, vol. 26, 1990, pp. 37–54.

[4] R. Rudolf, P. Mitschang, and M. Neitzel, "Induction heating of continuous carbon-fiber-reinforced thermoplastics," *Composite: Part A*, vol. 31, pp. 1191–1202, 2000.

[5] A. Todoroki, M. Tanaka, and Y. Shimamura, "Measurement of orthotropic electric conductance of CFRP laminates and analysis of the effect on delamination monitoring with an electric resistance change method," *Comp. Sci. Technol.*, vol. 62, pp. 619–628, 2002.

[6] C. Guerin, G. Tanneau, and T. Ngneugueu, "A shell element for computing 3D eddy currents—Application to transformers," *IEEE Trans. Magn.*, vol. 1, no. 3, pp. 1360–1363, May 1995.

[7] N. É Angelidis, N. Khemiri, and P.-E. Irving, "Experimental and finite element study of the electrical potential technique for damage detection in CFRP laminates," *Smart Mater. Struct.*, vol. 14, pp. 147–154, 2005.

[8] G. Mook, R. Lange, and O. Koeser, "Non-destructive characterization of carbon-fiber-reinforcement plastics by means of eddy currents," *Comp. Sci. Technol.*, vol. 61, pp. 865–873, 2000.

[9] A. Todoroki, M. Tanaka, and Y. Shimamura, "Electrical resistance change method for monitoring delaminations of CFRP laminates: Effect of spacing between electrodes," *Comp. Sci. Technol.*, vol. 65, no. 1, pp. 37–46, 2005.

Manuscript received June 26, 2005 (e-mail: samir.bensaid@ireena.univ-nantes.fr).